An Investigation of Simple Harmonic Oscillations of a Damped System

by: Alex Diep

Date: March 20, 2023

Instructor	Lisa Kinsale
TAs	Ahmed Elsherbiny
	Marjan Darabi
Group Members	Ahmad, Safiya
	Allegretto, Luca
	Colabella, James
	Dadhania, Karan
	Sammam, S M Faiaz
CCID	abdiep
Student ID	1664334
Section	H41
Group	13

1 Abstract

Vibrations are an incredibly important design consideration for several different systems and structures, and often requires thorough analysis. If not properly considered, damage or even catastrophic failure can occur. This lab was conducted to analyze a single degree of freedom spring cart system undergoing free, forced, and damped vibrations.

Load-deflection data was used to determine the effective stiffness, k_e, of the system. The effective stiffness was found to be 13.5 ± 0.2 N/m, with a coefficient of determination $R^2 = 0.9998$. The natural frequencies, p, were determined using k_e and the effective mass, m_e, of the system. The natural frequencies obtained were as follows: $p_{\text{small, sys}} = 1.1355$ Hz, $p_{\text{small, no sys}} = 0.9221$ Hz, $p_{\text{big, sys}} = 0.8744$ Hz, and $p_{\text{big, no sys}} = 0.7651$ Hz.

Next, free vibration data was used to experimentally determine the natural frequencies of the system. The natural frequencies obtained were as follows: $p_{\text{small, sys}} = 1.1317 \pm 0.013$ Hz, $p_{\text{small, sys}} = 0.9096 \pm 0.009$ Hz, $p_{\text{big, sys}} = 0.8576 \pm 0.012$ Hz, and $p_{\text{big, no sys}} = 0.7513 \pm 0.016$ Hz. The natural frequencies derived from the free vibration data were within 2% of the theoretical values derived from the effective stiffness and effective mass.

The average damping ratio, ζ, of the system was calculated from the decaying oscillations observed in the free vibration data. The damping ratio for the small cart was found to be $\zeta_{\text{small}} = 0.025$ and for the big cart was found to be $\zeta_{\text{big}} = 0.018$. The linear viscous damping model provided a reasonable approximation of the system's behavior when the amplitude was large, but became less accurate as the amplitude decreased.

A forced vibration test was performed to determine the dynamic magnification factor (DMF) of the system. The DMF closely followed theoretical expectations, with slight deviations observed, particularly in the out-of-phase region. The effects of the pulley measurement system on the natural frequency calculation were examined by considering the inertia of the pulleys. The effective mass of the system was determined from free vibration data, with the effective mass being found to be 0.4099 ± 0.009 kg for the small cart and 0.5818 ± 0.020 kg for the big cart. This had a relative error of 2.09% for the small cart and 0.25% for the big cart. The effective mass was found to be higher than the theoretical value, which could be due to neglecting the mass of the springs and cables, and other inertial effects.

Overall, the purpose of this lab was fulfilled, and the theory was experimentally tested and calculated experimentally in this lab report. General agreement was found between the theoretical and experimental results, with some discrepancies that could be improved through more comprehensive modelling.

Contents

List of Figures

List of Tables

2 Nomenclature

Table 1: Nomenclature

Symbol	Description
a	Initial Position
b	Final Position
c	Damping Coefficient
d	Deflection
DMF	Dynamic Magnification Factor
F	Force
J	Mass Moment of Inertia
k_e	Equivalent Stiffness
m	Cart Mass
m_1	Small Pulley Mass
m_2	Large Pulley Mass
m_e	Effective Mass
p	Natural Frequency
r	Inner Pulley Radius
R	Outer Puller Radius
ζ	Damping ratio

3 Introduction

Vibrations are ubiquitous in mechanical systems, manifesting in various scenarios such as pendulums, strings on pulleys, and ground-level buildings [1]. Identifying and understanding these vibrations is crucial for ensuring the safety and structural integrity of objects and materials in use. Vibrations can generally be categorized into forced and free types. Forced vibrations persist due to external forces acting on the system throughout the oscillation period, while free vibrations gradually lose energy over time [2]. In this laboratory experiment, both forced and free vibration setups are explored using single degree of freedom (SDOF) systems, serving as close approximations to real-life scenarios.

This lab report aims to explore fundamental vibration theories through experimentation on free and forced responses of small and large masses. The primary objectives include obtaining experimental values for parameters such as damping ratio, natural frequency, and dynamic magnification factor (DMF), while also investigating the effects of pulleys and comparing experimental results to theoretical predictions. Understanding the impacts of free and forced vibrations on mechanical systems is crucial for various engineering applications.

The experimentation begins with the calculation of the effective spring constant by attaching various weights to a cart and measuring displacement for each additional mass added. Subsequently, damping ratio and natural frequency are determined through free vibration trials. The theoretical natural frequency is derived from the spring constant and cart masses, while the experimental natural frequency is calculated by counting the number of cycles the cart undergoes within a specific time frame during free vibration. The calculated damping ratio is compared to the linear viscous damping model to assess its ability to represent energy dissipation in the air track system.

Next, DMF values are calculated during forced vibration tests. Experimental DMF data is collected using a data acquisition system (DAS), where the system undergoes vibrations at four frequencies both higher and lower than the resonance. The experimental DMF data is then compared to theoretical DMF values to analyze their correspondence during in-phase and 180 out-of-phase periods.

Further analysis involves calculating the forces acting on the mass cart and pulley using free-body diagrams. These force equations allow for corrections to the natural frequency values by adjusting the main mass values. Finally, the masses of the large and small pulleys are calculated and compared to nominal values.

The structure of this lab report includes detailed descriptions of the experimental procedure and equipment used, followed by a theoretical background section and analytical results and discussions on the findings. The report concludes with a summary of findings and technical recommendations for improving the experiment in the future.

4 Procedure

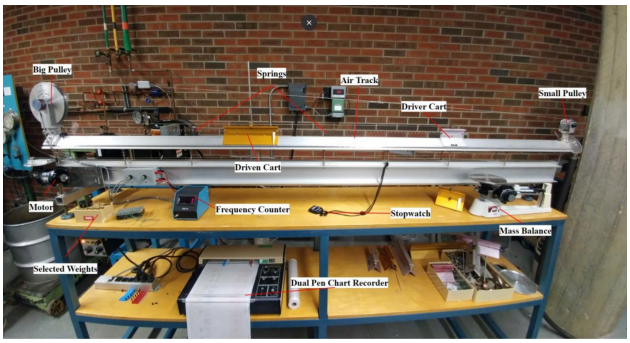

Figure 1: Experimental Setup of the Spring-Mass System

4.1 Equipment

- Air track, to provide a low friction surface for the carts
- Two springs, to provide an oscillatory response as the cart is displaced or driven
- Frequency counter, to measure the frequency of the forcing motor
- A large and small cart, to test the system with different masses
- Mass balance, to weigh the carts
- Motor and driver cart, to simulate a forced vibration system
- Pulleys, to record oscillations using software
- Stopwatch, to record the time of 10 oscillations
- Chart recorder, to record the oscillations of the system (not used in this experiment, software was used instead)
- Weights, to add to the cart to determine the load-deflection relationship of the system
- A pan, to hold the weights
- Vernier calipers, to measure the diameter of the pulley
- Data acquisition software, to record the oscillations of the system

4.2 Procedure

4.2.1 Load Deflection Trial

1. Record the mass of the cart by using the mass balance. Balance the beam by increasing and decreasing the weights on the other side of the beam until the beam is level. The mass of the cart will be used to determine the effective mass of the system for natural frequency calculations.
2. Set the driving cart to a fixed position (i.e. undriven). This will reduce the system to a single degree of freedom.

3. Detach the measurement system from the cart. This will allow the cart to oscillate freely.
4. Turn on the air track to reduce friction between the cart and the track.
5. Attach the cart to the pan around the free pulley. This will allow the cart to oscillate freely.
6. Record the initial position of the cart. This will be used to determine the deflection of the cart.
7. Add a 50 g weight to the pan. Record the new position of the cart. This will be used to determine the deflection of the cart.
8. Repeat steps 7 and 8, increasing by 50 g until 300 g of weight is reached. This will be used to determine the load-deflection relationship and determine the effective stiffness of the system.

4.2.2 Free Vibrations

1. Remove the weights from the pan. This will allow the cart to oscillate freely.
2. Give the cart an 10cm initial deflection and then release it. This will allow the cart to oscillate freely.
3. Record the time for the cart to complete ten oscillations using the stopwatch. This will be used to determine the natural frequency of the system.
4. Repeat steps 2 and 3 five times to get an average value. This will be used to determine the natural frequency of the system.
5. Redo steps 1-4 for the second, larger cart. This will be used to determine the natural frequency of the system for the larger cart.

4.2.3 Forced Vibrations

1. Attach the measurement system to the cart. This will allow the software to record the position of the cart.
2. Attach the driving cart to the motor. This will allow the motor to drive the system.
3. Turn on the motor and set the frequency below the determined natural frequency. This will allow the system to oscillate at a frequency below the natural frequency.
4. Once steady state is reached, record the oscillations using the software for about 20 seconds. This will be used to determine the dynamic response of the system.
5. Repeat steps 3 and 4 for four trials below the natural frequency and four trials above. This will be used to determine the dynamic response of the system.
6. Redo steps 3-5 for the second, larger cart. This will be used to determine the dynamic response of the system for the larger cart.

5 Theory

5.1 Free Vibrations

The experimental setup for free vibrations is modelled in Figure 2. The system consists of a mass m_e attached to a spring with stiffness k_e.

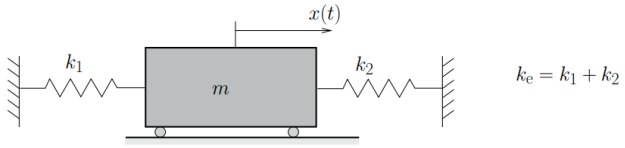

Figure 2: Spring-Mass System

If x is the displacement of the mass from its equilibrium position, the equation of motion is given by

$$m_e\ddot{x} + k_e x = 0 \tag{1}$$

The solution to Equation 1 is given by

$$x(t) = \frac{v_0}{p}\sin(pt) + x_0\cos(pt) \tag{2}$$

where v_0 is the initial velocity, x_0 is the initial displacement, and $p = \sqrt{\frac{k_e}{m_e}}$ is the natural frequency of the system. The natural frequency is the frequency at which the system will oscillate if it is displaced and released. The period of the system is given by

$$\tau = \frac{2\pi}{p} \tag{3}$$

5.2 Forced Vibrations

The experimental setup for forced vibrations is modelled in Figure 3. The system consists of a mass m_e attached to a spring with stiffness k_e. The force is $F(t) = kY_0\sin(\omega t)$.

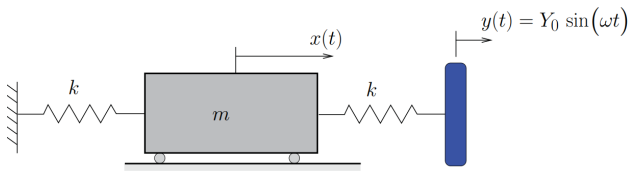

Figure 3: Forced Damped Vibrations System

The equation of motion for the system is given by

$$m_e\ddot{x} + k_e x = F_0 \cos(\omega t) \tag{4}$$

where $F_0 = kY_0$. The time-dependent solution to Equation 4 is

$$x(t) = \frac{Y_0}{2}\left[\frac{1}{1-\left(\frac{\omega}{p}\right)^2}\right]\sin(\omega t) \tag{5}$$

$$\tag{6}$$

where $p = \sqrt{\frac{k_e}{m_e}}$ is the natural frequency of the system. The DMF is given by

$$\text{DMF} = \frac{1}{\left|1-\left(\frac{\omega}{p}\right)^2\right|} \tag{7}$$

Plotting the DMF against ω/p will give the frequency response of the system, as shown in Figure 4. At $\omega/p < \sqrt{2}$, the DMF > 1, which means the system amplifies the input force. At $\omega/p > \sqrt{2}$, the DMF < 1, which means the system attenuates the input force. The system is in resonance at $\omega/p = 1$. Defining static deflection as

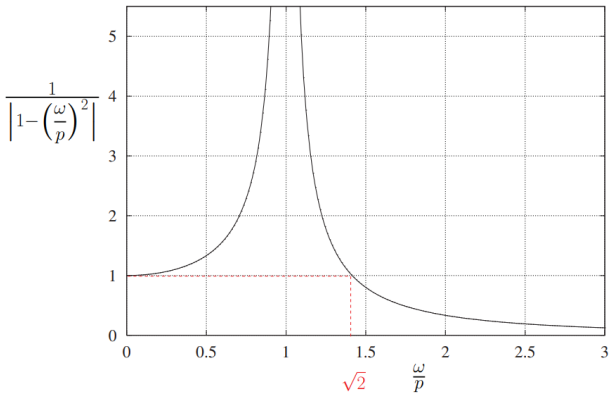

Figure 4: DMF vs. ω/p

$$\mathbb{X}_0 = \frac{F_0}{k_e} \tag{8}$$

we can see that the $Y_0/2$ term in Eq. 5 is static deflection.

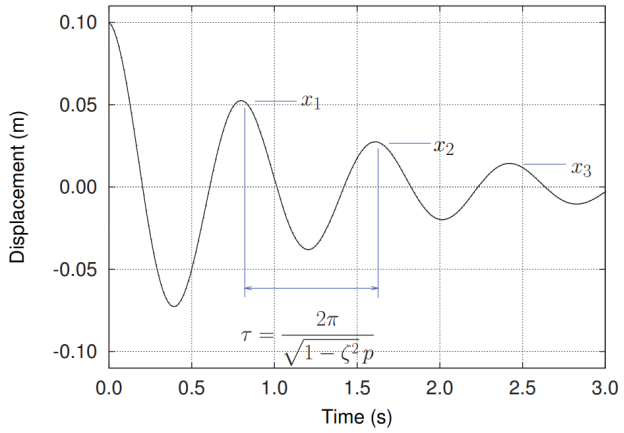

Figure 5: Damped Response of a Spring-Mass System

5.3 Damped Spring Mass System

An energy dissipation method is added to the system to model the energy loss in the system. The most common approach is to add viscous damping, which is proportional to the velocity of the mass. The equation of motion from Eq. 1 is modified to include damping as

$$m_e\ddot{x} + c_e\dot{x} + k_e x = 0 \tag{9}$$

where c_e is the damping coefficient. Assuming the mass is given an initial displacement and zero initial velocity, the solution to Eq. 9 is given by

$$x(t) = Ae^{\zeta t}\cos\left(\sqrt{1-\zeta^2}t\right) \tag{10}$$

where,

$$\zeta = \frac{c_e}{2m_e p} = \frac{c_e}{2\sqrt{k_e m_e}} \tag{11}$$

The solution to Eq. 9 is a decaying sinusoidal function, plotted in Figure 5. It can be shown that the peaks can be related by

$$\delta = \ln\left(\frac{x_n}{x_{n+1}}\right) = \frac{2\pi}{\sqrt{1-\zeta^2}} \tag{12}$$

From which, the damping ratio can be determined as

$$\zeta = \frac{\delta}{\sqrt{4\pi^2+\delta^2}} \tag{13}$$

5.4 Equivalent Mass of Measurement System

A schematic of the measurement system is shown in Figure 6. The equivalent mass of the system is given by

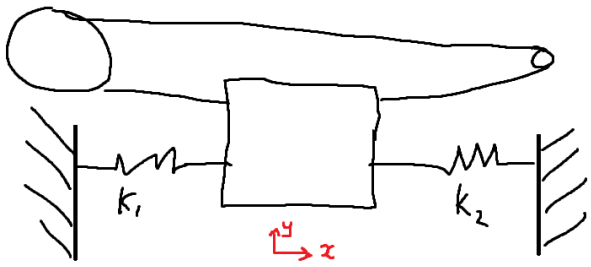

Figure 6: Cart and Pulley Measurement System

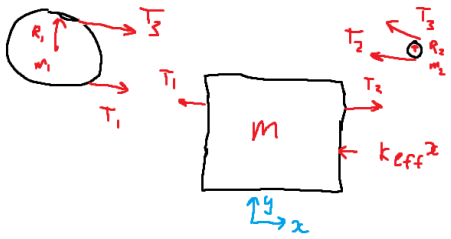

Figure 7: Free Body Diagram of the Cart and Pulleys

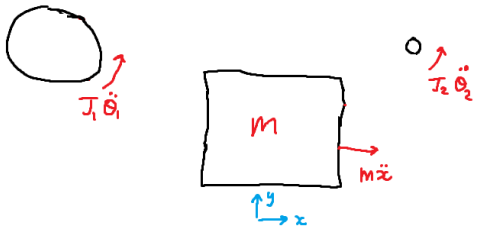

Figure 8: Mass Acceleration Diagram of the Cart and Pulleys

Taking the sum of forces in x, the moment about pulley 1's and pulley's 2 mass center,

$$\begin{aligned} \rightarrow \sum F_x &:= m_{\text{cart}}\ddot{x} \\ &= T_2 - T_1 - k_{\text{eff}}x \end{aligned} \tag{14}$$

$$\begin{aligned} \circlearrowleft \sum M_{\text{pulley 1}} &:= J_1\ddot{\theta}_1 \\ &= R_1(T_1 - T_3) \end{aligned} \tag{15}$$

$$\begin{aligned} \circlearrowleft \sum M_{\text{pulley 2}} &:= J_2\ddot{\theta}_2 \\ &= R_2(T_3 - T_2) \end{aligned} \tag{16}$$

Assuming the cable does not slip,

$$\theta_1 = \frac{\ddot{x}}{R_1}, \quad \theta_2 = \frac{\ddot{x}}{R_2} \tag{17}$$

Since the disks are uniform disks,

$$J_1 = \frac{1}{2}m_1R_1^2, \quad J_2 = \frac{1}{2}m_2R_2^2 \tag{18}$$

Combining Eq. (14), (15), (16) and using Eq. (17) and (18), we get

$$\underbrace{\left(m_{\text{cart}} + \frac{1}{2}m_1 + \frac{1}{2}m_2\right)}_{m_e}\ddot{x} + k_{\text{eff}}x = 0 \tag{19}$$

where m_e is the equivalent mass of the system. A full derivation is shown in Appendix E.

6 Results and Discussion

6.1 Effective Stiffness From Load-Deflection Data

The effective stiffness was determined to be 13.5 ± 0.2 N/m. The effective stiffness was determined by measuring the deflection of the spring under a various known masses under gravitational force. The results of the trial as well as the linear regression forced through the origin can be seen in Figure 9. The plot was forced through the origin since zero force should be observed at zero deflection. The coefficient of determination was found to be $R^2 = 0.9998$, which indicates a strong linear relationship between force and deflection.

From Hooke's, law, the slope of Figure 9 is the effective stiffness of the spring, which was found to be 13.5 N/m. The spring stiffness should be independent of the cart masses as well as the measurement system.

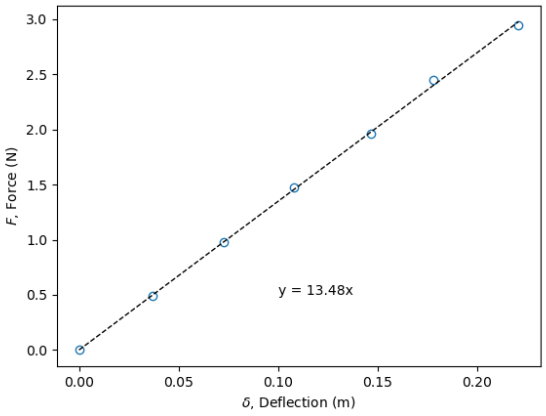

Figure 9: Force vs. Deflection

6.2 Experimental Resonance

Table 2: Natural Frequency Data

	Small		Big	
	f_{sys} (Hz)	$f_{\text{no sys}}$ (Hz)	f_{sys} (Hz)	$f_{\text{no sys}}$ (Hz)
Derived from period	1.1317 ± 0.013	0.9096 ± 0.009	0.8576 ± 0.012	0.7513 ± 0.016
Derived from using k_e and m_e	1.1355	0.9221	0.8744	0.7651
Relative error (%)	0.3286	1.3536	1.9203	1.7989

The natural frequencies of the mass-cart with and without measurement system for experimental and theoretical values are shown in Table 2.The period of 10 cycles was determined experimentally by displacing the mass and measuring the time it took to complete 10 cycles. Details of the analysis can be found in Appendix B. The natural frequency of the system was found to be 1.1317 ± 0.013 Hz for the small cart with the measurement system, 0.9096 ± 0.009 Hz for the small cart without the measurement system, 0.8576 ± 0.012 Hz for the big cart with the measurement system, and 0.7513 ± 0.016 Hz for the big cart without the measurement system.

The theoretical natural frequencies were calculated using the effective stiffness and effective mass. Effective stiffness was found to be k_e = 13.5 ± 0.2 N/m, and the effective mass was found by using Eq. (19), as summarized in Table 4. The theoretical natural frequencies were found to be 1.1355 Hz for the small cart with the measurement system, 0.9221 Hz for the small cart without the measurement system, 0.8744 Hz for the big cart with the measurement system, and 0.7651 Hz for the big cart without the measurement system.

The experimental natural frequencies were found to be within 0.3286% to 1.9203% of the theoretical values. The theoretical values were slightly higher than the experimental values, which could be due to neglecting the mass of the spring and the mass of the cable. In addition, the experimental period calculations neglected the effects of damping, which would would impact the calculation of the natural frequency.

6.3 Damping Ratio

The time response of the amplitude of the small and big carts can be seen in Figures 10, 11, 12, and 13. The damping ratio was calculated using the logarithmic decrement method (Eq. 13) and shown in Appendix C. The average damping ratio was taken from the linear region (first 6 cycles) as

shown in Figures 14 and 15. The average damping ratios were found to be $\zeta_{\text{small},1,2} = 0.021, 0.016$ and $\zeta_{\text{big},1,2} = 0.027, 0.023$.

The discrepancy between the two damping ratios obtained for each trial is due to the non-linear nature of the damping in the system as it approached small amplitudes. The theory suggests, for a linear viscous damping model, that the damping ratio would remain constant, independent of the cycle. From Figures 14 and 15, the damping ratio was found to change nearly every cycle, increasing exponential-like. This is not consistent with the linear viscous damping model. The linear viscous damping model does not accurately represent the energy dissipation in the air track system at small amplitudes.

Further work could be done in displacing the cart by a larger amplitude to see if the damping ratio remains constant initially. Other effects that could be considered are the effects of friction from the air track, torsional friction in the pins of the pulleys, and the mass of the springs and cables.

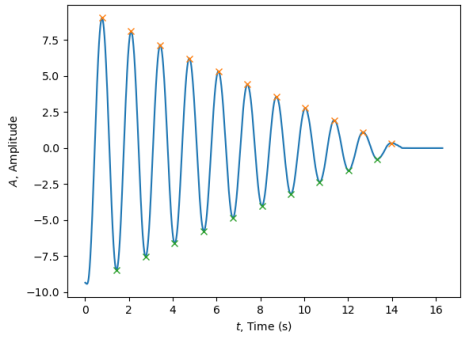

Figure 10: Big Cart Amplitude vs. Time for Trial 1

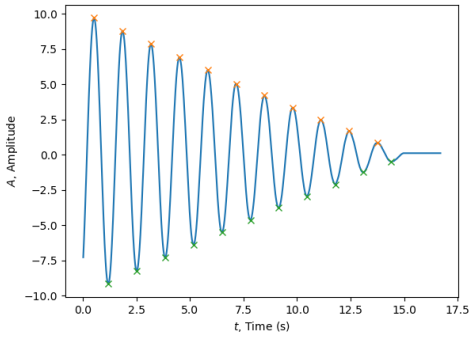

Figure 11: Big Cart Amplitude vs. Time for Trial 2

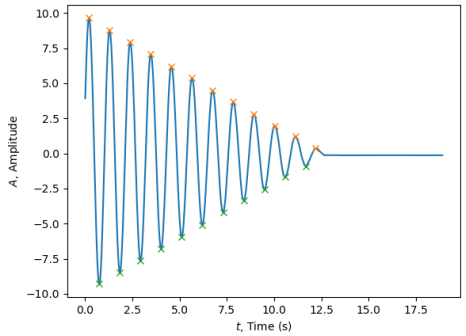

Figure 12: Small Cart Amplitude vs. Time for Trial 1

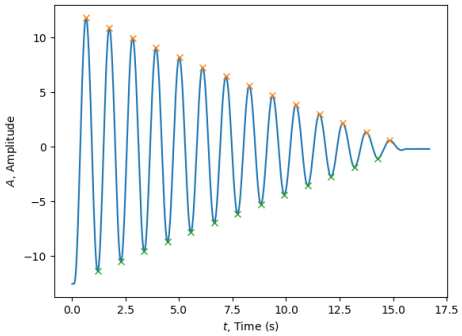

Figure 13: Small Cart Amplitude vs. Time for Trial 2

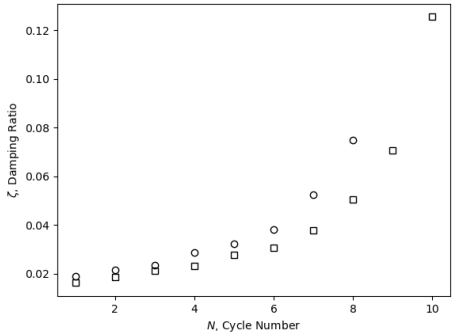

Figure 14: Big Cart Damping Ratio Vs. Cycle Number

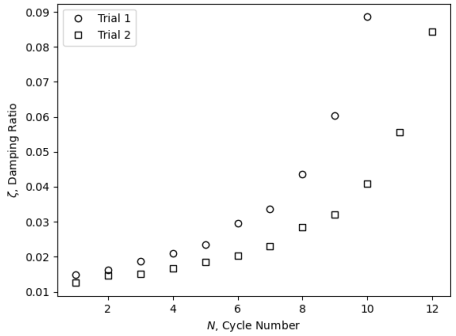

Figure 15: Small Cart Damping Ratio Vs. Cycle Number

6.4 Dynamic Magnification Factor

The dynamic magnification factor was calculated using the measured displacements for both masses and plotted against the frequency ratio ω/p as shown in Figures 16 and 17. This plot was made from the forced response of the system experiment, which tested the response at four forcing frequencies and constant amplitude, $Y_0 = 3.55\,\text{cm}$.

The DMF follows the theoretical curve closely, with the in-phase region being very close to the theory. The out-of-phase region was slightly off, with the amplitude being smaller than expected. This could be due to neglecting some inertial terms, such as the mass of the springs and cables as well as the torsional friction in the pins of the pulleys or the friction from the air track. It also can be noted that the DMF is less than one after $\omega/p = \sqrt{2}$, which follows the theory. More details on the analysis can be found in Appendix D.

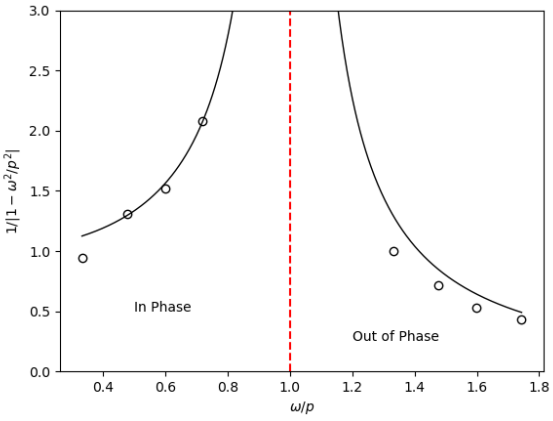

Figure 16: Big Cart DMF vs. ω/p

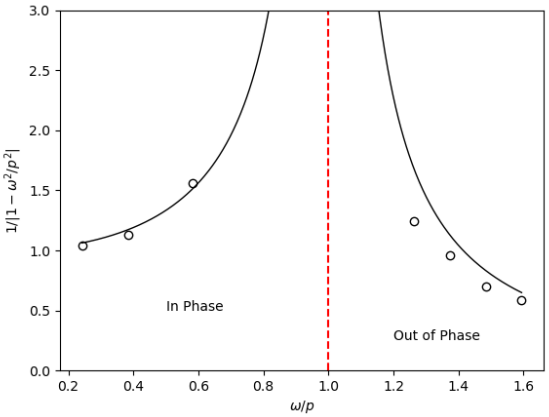

Figure 17: Small Cart DMF vs. ω/p

6.5 Effects of Pulley Measurement System

The diagram of the pulley system was shown in the theory, Section 5.4. Assuming the pulley is a uniform disk, the effective mass, m_e, was found to be $m_e = m_{\text{cart}} + 0.5m_{\text{pulley 1}} + 0.5m_{\text{pulley 2}}$. The partial derivation was shown in Section 5.4, with the full derivation shown in Appendix E.

Table 3: Effective Mass Data

	Small (kg)	Big (kg)
Cart	0.2648	0.4465
Pulley	0.2599	0.0136

Table 4: Effective Mass Data

	System (kg)	No System (kg)
m_e, Small	0.40155	0.2648
m_e, Big	0.58325	0.4465

The pulleys and carts were measured by a mass balance. The masses are shown in Table 3. The effective mass of the system was found to be $m_e = 0.40155$ kg for the small cart with the

measurement system, 0.2648 kg for the small cart without the measurement system, 0.58325 kg for the big cart with the measurement system, and 0.4465 kg for the big cart without the measurement system.

The effective mass of the system was found to be higher with the measurement system, which is expected since the pulleys add mass to the system. The inertial effects of the pulley system adds 0.1368 kg to the effective mass.

6.6 Effective Mass Derived From Free Vibration

From the free vibration data, as shown in Table 2, the effective mass was derived using the natural frequencies of the system. The effective mass was found to be 0.4099 kg for the small cart and 0.5818 kg for the big cart. The theoretical effective mass was found to be 0.4016 kg for the small cart and 0.5833 kg for the big cart. The relative error was found to be 2.09% for the small cart and 0.25% for the big cart. The effective mass was found to be within 2.09% of the theoretical value for the small cart and 0.25% for the big cart. The effective mass was found to be higher than the theoretical value, which could be due to neglecting the mass of the springs and cables, and other inertial effects such as the friction from the air track and the torsional friction in the pins of the pulleys.

Table 5: Effective Mass Data

	Small Cart (kg)	Big Cart (kg)
Effective Mass from Trials	0.4099 ± 0.009	0.5818 ± 0.020
Effective Mass from Theory	0.4016	0.5833
Relative Error	2.09%	0.25%

7 Conclusion

This experiment served to analyze a single degree of freedom spring-cart system undergoing different forms of vibration. This analysis used data from free, forced, and damped vibration tests, and compared the results from these tests against their theoretical counterparts.

The effective stiffness, k_e, of the system was determined to be 13.5 ± 0.2 N/m, derived from the load-deflection data. This result was obtained through the application of known masses to the spring, with a coefficient of determination $R^2 = 0.9998$ for a linear line forced through the origin. The plot is consistent with Hooke's Law, which states that the force exerted by a spring is linearly

proportional to the displacement of the spring. The high coefficient of determination is evidence of the high linearity of the data.

The natural frequencies, p, were determined using k_e and the effective mass, m_e, of the system. The natural frequencies obtained were as follows: $p_{\text{small, sys}} = 1.1355$ Hz, $p_{\text{small, no sys}} = 0.9221$ Hz, $p_{\text{big, sys}} = 0.8744$ Hz, and $p_{\text{big, no sys}} = 0.7651$ Hz.

Next, the free vibration data was also used to determine the natural frequencies of the system by displacing the cart and measuring the time it takes to complete 10 full oscillations. The natural frequencies obtained were as follows: $p_{\text{small, sys}} = 1.1317 \pm 0.013$ Hz, $p_{\text{small, no sys}} = 0.9096 \pm 0.009$ Hz, $p_{\text{big, sys}} = 0.8576 \pm 0.012$ Hz, and $p_{\text{big, no sys}} = 0.7513 \pm 0.016$ Hz. These natural frequencies were derived from experimental measurements, comparing observed free vibration data with theoretical expectations. Overall, the experimental results closely matched the results obtained by using the effective stiffness and effective mass, being within 2% of the free vibration results.

The average damping ratio, ζ, of the system was calculated from the decaying oscillations observed in the free vibration data. Two trials were performed for both the small and big carts, without the measurement system attached. The damping ratio for the small cart was found to be $\zeta_{\text{small}} = 0.025$ and for the big cart was found to be $\zeta_{\text{big}} = 0.018$. Software was used to track the amplitude of the cart. These values were obtained by selecting several pairs of consecutive maxima along the oscillations away from the end of the oscillations. The damping ratio did not stay constant, which is not consistent with the linear viscous damping model. In fact, the damping ratio increased exponential-like as it approached rest. This could be due to non-linear damping effects, such as torsional friction in the pin, or friction in the air track. Generally, the linear viscous damping model provided a reasonable approximation of the system's behavior when the amplitude was large, but became less accurate as the amplitude decreased.

A forced vibration test was performed to determine the dynamic magnification factor (DMF) of the system. The DMF was calculated using the measured displacements for both masses, plotted against the frequency ratio ω/p. The DMF closely followed theoretical expectations, with slight deviations observed, particularly in the out-of-phase region. These discrepancies could be attributed to neglected inertial effects and friction in the system. However, overall, the agreement between theory and experiment was satisfactory.

The effects of the pulley measurement system on the natural frequency calculation were examined by considering the inertia of the pulleys. By drawing a free-body diagram and analyzing the system, it was determined that the effective mass of the system increased when the measurement system was attached. The relationship was determined to be $m_e = m_{\text{cart}} + 0.5m_{\text{pulley 1}} + 0.5m_{\text{pulley 2}}$. The addition of the pulleys adds an effective mass of 0.1368 kg to the system. The correction required in the natural frequency calculation highlighted the importance of accounting for inertial effects in experimental setups.

Finally, the effective mass of the system was determined from free vibration data. The effective mass was determined to be 0.4099 ± 0.009 kg for the small cart and 0.5818 ± 0.020 kg for the big cart. This was determined by comparing the natural frequency of the system with and without the measurement system attached. The effective mass determined by free vibration closely matched theoretical values derived from mechanics within a relative error of 2.09% for the small cart and 0.25% for the big cart. The low relative error indicates that the effective mass was determined accurately. The effective mass from the vibration data was found to be higher than the theoretical value, which could be due to neglecting the mass of the springs and cables, and other inertial effects such as the friction from the air track and the torsional friction in the pins of the pulleys. Overall, the experimental results provided valuable insights into the behavior of the system, emphasizing the importance of comprehensive analysis and consideration of all relevant factors in experimental design.

7.1 Technical Recommendations

The experiment was successful in determining the effective mass of the system. However, there are several areas where improvements could be made. The damping ratio was found to increase as the amplitude decreased, which is not consistent with the linear viscous damping model. Further investigation into the causes of damping fluctuations could provide valuable insights into system dynamics.

Additionally, the DMF was found to deviate slightly from theoretical expectations, particularly in the out-of-phase region. This discrepancy could be attributed to neglected inertial effects and friction in the system. Future experiments could focus on reducing these discrepancies by accounting for additional inertial effects and friction in the system.

The uncertainty of the natural frequency could be reduced by using an the data acquisition system to measure the time it takes to complete 10 cycles. This would reduce the uncertainty in the period calculation, which would reduce the uncertainty in the natural frequency calculation.

Finally, the effective mass was found to be higher than the theoretical value, which could be due to neglecting the mass of the springs and cables, and other inertial effects. Future experiments could aim to reduce this discrepancy by accounting for these additional inertial effects in the experimental setup.

8 References

[1] A. J. Wheeler and A. R. Ganji, *Introduction to engineering experimentation*, 3rd ed. Upper Saddle River, N.J: Pearson Higher Education, 2010, oCLC: ocn459211853.

A Appendix: Effective Stiffness from Load-Deflection Data

This appendix outlines the calculations used to determine the experimental effective stiffness of the system. The effective stiffness is determined by measuring the deflection of the spring under a known load. The stiffness was determined by a linear regression through the origin of the load-deflection data. The data is shown in Table A.6.

A.1 Effective Stiffness Calculation

Table A.6: Load-Deflection Data

Mass (g)	Force (N)	Initial Position, a (cm)	Final Position, b (cm)	Deflection, x (m)
0	0.000	91.1	91.1	0.00
50	0.491	91.1	87.4	0.0370
100	0.981	91.1	83.8	0.0730
150	1.47	91.1	80.3	0.108
200	1.96	91.1	76.4	0.147
250	2.45	91.1	73.3	0.178
300	2.94	91.1	69.0	0.221

Sample calculations for the effective stiffness are shown for the 50 g mass. The deflection was found by

The spring was subject to gravitational force from the applied mass. The force was found by

$$\begin{aligned} F &= mg \\ &= 50 \times 10^{-3}\,\text{kg} \times 9.81\,\text{m}\,\text{s}^{-2} \\ &= 0.491\,\text{N} \end{aligned}$$

The deflection was found by

$$\begin{aligned} x &= a - b \\ &= 91.1\,\text{cm} - 87.4\,\text{cm} \\ &= 0.0370\,\text{m} \end{aligned}$$

Next, a linear regression was applied to the data to determine the effective stiffness. From Excel,

Table A.7: Linear Regression Data

Parameter	Value
Spring constant, k_e	$13.5\,\mathrm{N\,m^{-1}}$
Standard error, S_k	$0.082\,\mathrm{N\,m^{-1}}$
R^2	0.9998

So, the effective stiffness of the spring is

$$\boxed{k_e = 13.5\,\mathrm{N\,m^{-1}}}$$

A.2 Effective Stiffness Error

A.2.1 Error Propagation Derivation

To be thorough, the error propagation formula will be derived for completeness.

If we know how a quantity of interest depends on other, directly measurable quantizes, it is posable to estimate the uncertainty of this "output" quantity based on the uncertainties in the measured quantizes. For example, we can calculate the uncertainty associated to a volume based on the uncertainty of the measurement of the individual dimensions.

Consider as results, R, which is a function of n variables, $x_1, \ldots, x_n$:

$$R = f(x_1, \ldots, x_n)$$

If the individual measurands, x_i, have an associated uncertainty w_{x_i}, what is teh uncertainty of w_R of the result R?

Defining $x := (x_1, \ldots, x_n)$, and $x_m := (x_{m,1}, \ldots, x_{m,n})$, perform the Taylor series expansion of $R = f(x)$ about the point $x = x_m$, taking $x_i - x_{m,i} = w_{x_i}$:

$$R = f(x_m) + \left.\frac{\partial f}{\partial x_1}\right|_{x=x_m} \underbrace{(x_1 - x_{m,1})}_{w_{x_1}} + \ldots + \left.\frac{\partial f}{\partial x_n}\right|_{x=x_m} \underbrace{(x_n - x_{m,n})}_{w_{x_n}} + \text{H.O.T.}$$

$$\underbrace{R - f(x_m)}_{w_R} = \left.\frac{\partial f}{\partial x_1}\right|_{x=x_m} w_{x_1} + \ldots + \left.\frac{\partial f}{\partial x_n}\right|_{x=x_m} w_{x_n} + \text{H.O.T.}$$

The higher-order terms contain quadratic terms $w_{x_i} w_{x_j}$, cubic terms $w_{x_i} w_{x_j} w_{x_k}$, and so on. As-

suming the individual uncertainties w_{x_i} are small, we can take these higher-order terms as zero, giving

$$w_R = \sum_{i=1}^{n} \left| \left. \frac{\partial f}{\partial x_i} \right|_{x=x_m} w_{x_i} \right|$$

However, this is the worst-case uncertainty, and is an overly conservative estimate. A better estimate is to use the root of sum of squares

$$w_R = \sqrt{\sum_{i=1}^{n} \left[\left. \frac{\partial f}{\partial x_i} \right|_{x=x_m} w_{x_i} \right]^2} \tag{20}$$

If the confidence levels associated to the individual uncertainties w_{x_i} are all identical (for instance 95%), the confidence level of the result w_R will be the same.

The key assumption behind RSS is that the set of measured variables $x_1, \ldots, x_n$ are **statistically indecent**. If this is not the case, a different formulation needs to be used. Also note that all uncertainties w_{x_i} need to be small such that the first-order Taylor series approximation holds.

Consider the case where the result R is dependent only on the product of the measured variables, $x_1, \ldots, x_n$ with associated uncertainties $w_{x_1}, \ldots, w_{x_n}$ as

$$R = C x_1^{c_1} x_2^{c_2} \ldots x_n^{c_n}$$

where C and $c_1, \ldots, c_n$ are constants. In this case, the RSS formula gives

$$\begin{aligned} w_R &= \sqrt{\left(C c_1 x_1^{c_1 - 1} w_{x_1} \right)^2 + \ldots + \left(C c_n x_1^{c_1} x_2^{c_2} \ldots c_n x_n^{c_n - 1} w_{x_n} \right)^2} \\ \implies \frac{w_R}{|R|} &= \sqrt{\left(\frac{c_1 w_{x_1}}{x_1} \right)^2 + \ldots + \left(\frac{c_n w_{x_n}}{x_n} \right)^2} \end{aligned} \tag{21}$$

Recall from MEC E 300 that the error for the coefficients for the form $f(x) = ax + b$ can be found by finding standard error of a and b by first finding

$$S_{y,x} = \sqrt{\frac{\sum (y_i - a x_i - b)^2}{n - 2}}$$

then,

$$S_a = S_{y,x}\sqrt{\frac{1}{\sum(x_i - \bar{x})^2}}$$
$$S_b = S_{y,x}\sqrt{\frac{\sum x_i^2}{n\sum(x_i - \bar{x})^2}}$$

then with a given confidence of $1 - \alpha$, the uncertainties are

$$a \pm t_{\alpha/2,n-2}S_a$$
$$b \pm t_{\alpha/2,n-2}S_b$$

The uncertainty of the slope is then [1]

$$w_a = t_{\alpha/2,n-2}S_a \tag{22}$$

A.2.2 Error Propagation for Effective Stiffness

Given a confidence level of 95%, the t-distribution value was determined by

$$\alpha/2 = \frac{1 - 0.95}{2} = 0.025$$
$$n - 2 = 7$$
$$t_{\alpha/2,n-2} = 2.5706$$

By Eq. (22), the error in the effective stiffness with a confidence level of 95% is

$$\begin{aligned}\delta_{k_e} &= t_{\alpha/2,n-2}S_k \\ &= 2.5706 \times 0.082\,\mathrm{N\,m^{-1}} \\ &= \boxed{0.21\,\mathrm{N\,m^{-1}}}\end{aligned}$$

B Appendix: Natural Frequency

B.1 Period Calculation

Table B.8: Natural Frequency Trial Data

	Small		Big	
Trial	$10\tau_{\text{no sys}}$ (s)	$10\tau_{\text{sys}}$ (s)	$10\tau_{\text{no sys}}$ (s)	$10\tau_{\text{sys}}$ (s)
1	8.81	11.13	11.49	13.7
2	8.71	10.98	11.67	13.14
3	8.85	11.01	11.69	13.31
4	8.88	10.90	11.84	13.19
5	8.93	10.95	11.61	13.21
Average	8.836	10.994	11.66	13.31
τ	0.8836	1.0994	1.166	1.331

The experimental data for the period of the system is shown in Table B.8. Sample calculations for the period are shown for the small no system trial. The average was found by Excel,

$$\begin{aligned}(10\tau_{\text{no sys}})_{\text{avg}} &= \frac{1}{5}\sum_{i=1}^{5}(10\tau_{\text{no sys}})_i \\ &= \frac{1}{5}\times(8.81+8.71+8.85+8.88+8.93) \\ &= 8.836\end{aligned}$$

The period was found by

$$\begin{aligned}\tau_{\text{no sys}} &= \frac{(10\tau_{\text{no sys}})_{\text{avg}}}{10} \\ &= \frac{8.836}{10} \\ &= \boxed{0.8836}\end{aligned}$$

B.2 Natural Frequency Calculation

Table B.9: Natural Frequency Data

	Small		Big	
	f_{sys} (Hz)	$f_{\text{no sys}}$ (Hz)	f_{sys} (Hz)	$f_{\text{no sys}}$ (Hz)
Derived from period	1.1317	0.9096	0.8576	0.7513
Derived from using k_e and m_e	1.1355	0.9221	0.8744	0.7651

Table B.10: Effective Mass Data

	System (kg)	No System (kg)
m_e, Small	0.40155	0.2648
m_e, Big	0.58325	0.4465

The natural frequency of the system was calculated using the period data in Table B.9. Sample calculations for the natural frequency are shown for the small system trial. The natural frequency was found by

$$\begin{aligned} f_{\text{sys}} &= \frac{1}{\tau_{\text{sys}}} \\ &= \frac{1}{1.0994} \\ &= \boxed{0.9096} \end{aligned}$$

The natural frequency was also calculated using the effective stiffness and mass data. The effective mass data is shown in Table B.10. The effective mass for the system was found by

$$\begin{aligned} m_{e,\text{sys}} &= m_{\text{cart}} + \frac{1}{2} m_{\text{big pulley}} + \frac{1}{2} m_{\text{small pulley}} \\ &= 0.2648\,\text{kg} + \frac{1}{2} 0.2599\,\text{kg} + \frac{1}{2} 0.0136\,\text{kg} \\ &= 0.40155\,\text{kg} \end{aligned}$$

The natural frequency was found by

$$\begin{aligned} f_{\text{sys}} &= \frac{1}{2\pi}\sqrt{\frac{k_e}{m_e}} \\ &= \frac{1}{2\pi}\sqrt{\frac{13.5\,\text{N m}^{-1}}{0.40155\,\text{kg}}} \\ &= \boxed{1.1355} \end{aligned}$$

B.3 Natural Frequency Error Analysis

Important values for uncertainty analysis are presented in Table B.9. Sample calculations for the

Table B.11: Natural Frequency Error Analysis

	Small		Big	
	w/ sys	w/o sys	w/ sys	w/o sys
Stdev 10τ (s)	0.0829	0.0862	0.1273	0.2266
t-inv value	2.7764	2.7764	2.7764	2.7764
$P_{10\tau}$ (s)	0.1030	0.1070	0.1580	0.2814
$B_{10\tau}$ (s)	0.01	0.01	0.01	0.01
δ_τ (s)	0.0103	0.0107	0.0158	0.0281
δ_p (Hz)	0.013	0.009	0.012	0.016

error analysis are shown for the small system trial. The standard deviation was calculated by Excel. The precision error for 10τ was found by

$$\begin{aligned} P_{10\tau} &= t_{\alpha/2,n-1} \times \frac{\text{stdev } 10\tau}{\sqrt{n}} \\ &= 2.7764 \times \frac{0.0829}{\sqrt{5}} \\ &= 0.1030 \end{aligned}$$

where $t_{\alpha/2,n-1} = 2.7764$ for a 95% confidence interval. The bias error for τ was set to be the resolution of the stopwatch. Next, the uncertainty for 10τ was found by

$$\begin{aligned}\delta_\tau &= \sqrt{P_{10\tau}^2 + B_{10\tau}^2} \\ &= \sqrt{0.1030^2 + 0.01^2} \\ &= 0.0103\,\text{s}\end{aligned}$$

The uncertainty for τ was found by

$$\begin{aligned}\delta_p &= \sqrt{\left(\frac{\partial 10\tau}{10}\delta_\tau\right)^2} \\ &= \frac{1}{10}\delta_\tau \\ &= \frac{0.0103}{10} \\ &= \boxed{0.0010}\end{aligned}$$

Lastly, $p = \frac{1}{\tau} = \tau^{-1}$. Since this is the special multiplicative case as derived in Eq. (21),

$$\begin{aligned}\delta_p &= p\frac{\delta_\tau}{\tau} \\ &= 0.9096 \times \frac{0.0103}{1.0994} \\ &= \boxed{0.013}\end{aligned}$$

C Appendix: Damping Ratio

C.1 Damping Ratio Calculation

Table C.12: Damping Ratio Data

Dataset	Peak Number	Amplitude, x (cm)	δ	ζ
Big 1	1	8.2775	0.119385043	0.018997291
Big 1	2	7.346	0.134348497	0.021377341
Big 1	3	6.4225	0.146730503	0.02334652
Big 1	4	5.546	0.179764425	0.028598694
Big 1	5	4.6335	0.202002469	0.032133089
Big 1	6	3.786	0.240058119	0.038178581
Big 1	7	2.978	0.328811927	0.052260531
Big 1	8	2.1435	0.471264045	0.074793917
Big 1	9	1.338	-	-
Big 2	1	9.4465	0.101586118	0.01616582
Big 2	2	8.534	0.116963123	0.018612035
Big 2	3	7.592	0.132252668	0.021044005
Big 2	4	6.6515	0.145034028	0.023076735
Big 2	5	5.7535	0.17320361	0.027555743
Big 2	6	4.8385	0.192437655	0.030613049
Big 2	7	3.9915	0.23835321	0.037907825
Big 2	8	3.145	0.317698849	0.05049883

Dataset	Peak Number	Amplitude, x (cm)	δ	ζ
Big 2	9	2.289	0.444895542	0.070630487
Big 2	10	1.467	0.79495422	0.125520247
Big 2	11	0.6625	-	-
Small 1	1	9.473	0.093317023	0.014850228
Small 1	2	8.629	0.102608739	0.016328511
Small 1	3	7.7875	0.118031863	0.018782041
Small 1	4	6.9205	0.131541363	0.020930872
Small 1	5	6.0675	0.147293322	0.023436022
Small 1	6	5.2365	0.185362555	0.029488537
Small 1	7	4.3505	0.211971847	0.033717185
Small 1	8	3.5195	0.27362217	0.043507086
Small 1	9	2.677	0.379561461	0.060299159
Small 1	10	1.8315	0.55872893	0.088574955
Small 1	11	1.0475	-	-
Small 2	1	23.182	0.078630971	0.012513528
Small 2	2	21.429	0.091411866	0.014547111
Small 2	3	19.557	0.095540303	0.015203954
Small 2	4	17.775	0.10451699	0.016632095
Small 2	5	16.011	0.1158877	0.018440964
Small 2	6	14.259	0.126950746	0.020200716
Small 2	7	12.559	0.144982969	0.023068616

Dataset	Peak Number	Amplitude, x (cm)	δ	ζ
Small 2	8	10.864	0.178279663	0.028362675
Small 2	9	9.09	0.201245362	0.032012778
Small 2	10	7.433	0.257773714	0.040991478
Small 2	11	5.744	0.350674281	0.055724823
Small 2	12	4.045	0.532063149	0.084378491
Small 2	13	2.376	-	-

The raw data for the damping ratio calculation is shown in Table C.12. Sample calculations for the damping ratio are shown for the Big 1 dataset. First, δ was found by

$$\begin{aligned}\delta &= \ln\left(\frac{x_n}{x_{n+1}}\right)\\ &= \ln\left(\frac{8.2775}{7.346}\right)\\ &= 0.119385043\end{aligned}$$

Then, ζ was found by

$$\begin{aligned}\zeta &= \frac{\delta}{\sqrt{4\pi^2+\delta^2}}\\ &= \frac{0.119385043}{\sqrt{4\pi^2+0.119385043^2}}\\ &= \boxed{0.018997}\end{aligned}$$

D Appendix: Dynamic Magnification Factor

Table D.13: Dynamic Magnification Factor Data

Dataset	Frequency (Hz)	DMF	$\frac{f}{p}$	Mean Amplitude, A
Small 0.22 Hz	0.22	1.0396	0.2419	1.8454
Small 0.35 Hz	0.35	1.1287	0.3848	2.0034
Small 0.53 Hz	0.53	1.5598	0.5827	2.7686
Small 1.15 Hz	1.15	1.2427	1.2643	2.2057
Small 1.25 Hz	1.25	0.9588	1.3743	1.7019
Small 1.35 Hz	1.35	0.7020	1.4842	1.2460
Small 1.45 Hz	1.45	0.5868	1.5941	1.0417
Big 0.25 Hz	0.25	0.9437	0.3328	1.6751
Big 0.36 Hz	0.36	1.3088	0.4792	2.3231
Big 0.45 Hz	0.45	1.5176	0.5990	2.6937
Big 0.54 Hz	0.54	2.0809	0.7187	3.6937
Big 1.00 Hz	1.00	1.0029	1.3310	1.7801
Big 1.11 Hz	1.11	0.7129	1.4774	1.2654
Big 1.20 Hz	1.20	0.5327	1.5972	0.9455
Big 1.31 Hz	1.31	0.4284	1.7436	0.7605

Sample calculations for the dynamic magnification factor are shown for the small 0.22 Hz dataset. The mean amplitude was found by Excel by averaging the amplitudes across the number of cycles. The dynamic magnification factor was found by

$$\begin{aligned} \text{DMF} &= \frac{2 \times A}{Y_0} \\ &= \frac{2 \times 1.8454\,\text{cm}}{3.55\,\text{cm}} \\ &= \boxed{1.0396} \end{aligned}$$

The ratio of the frequency to the experimental natural frequency was found by

$$\begin{aligned}\frac{f}{p} &= \frac{0.22\,\text{Hz}}{0.909587047\,\text{Hz}} \\ &= \boxed{0.2419}\end{aligned}$$

where Y_0 is 3.55 cm

E Appendix: Equivalent Mass

This appendix outlines the calculations used to determine the equivalent mass of the measurement system. The equivalent mass is determined by analyzing the forces and moments acting on the system. The system is shown in Figure 6.

A schematic of the measurement system is shown in Figure 6. The equivalent mass of the system is given by

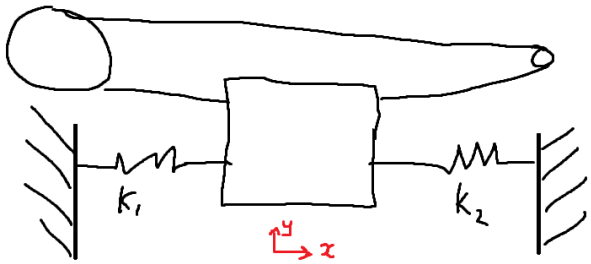

Figure E.18: Cart and Pulley Measurement System

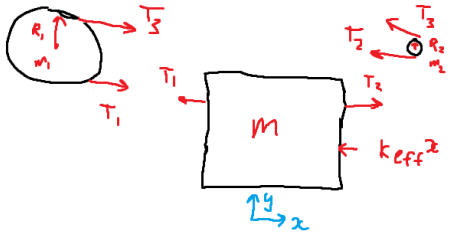

Figure E.19: Free Body Diagram of the Cart and Pulleys

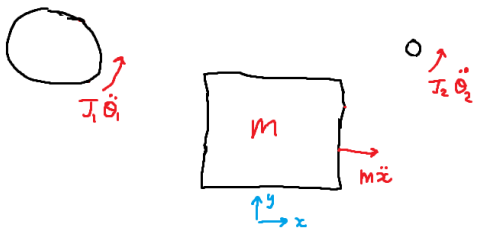

Figure E.20: Mass Acceleration Diagram of the Cart and Pulleys

Taking the sum of forces in x, the moment about pulley 1's and pulley's 2 mass center,

$$\begin{aligned} \rightarrow \sum F_x &:= m_{\text{cart}}\ddot{x} \\ &= T_2 - T_1 - k_{\text{eff}}x \end{aligned} \tag{23}$$

$$\begin{aligned} \circlearrowleft \sum M_{\text{pulley 1}} &:= J_1\ddot{\theta}_1 \\ &= r_1(T_1 - T_3) \end{aligned} \tag{24}$$

$$\begin{aligned} \circlearrowleft \sum M_{\text{pulley 2}} &:= J_2\ddot{\theta}_2 \\ &= r_2(T_3 - T_2) \end{aligned} \tag{25}$$

Assuming the cable does not slip in the the grooves of the pulleys at radius r_1 and r_2,

$$\theta_1 = \frac{\ddot{x}}{r_1}, \quad \theta_2 = \frac{\ddot{x}}{r_2} \tag{26}$$

Next, combining Eq. (23), (24), (25) and using Eq. (26), we get

$$\begin{aligned} J_1 \frac{\ddot{x}}{r_1} &= r_1(T_1 - T_3) \\ \implies \frac{J_1}{r_1^2}\ddot{x} &= T_1 - T_3 \end{aligned} \tag{27}$$

$$\begin{aligned} J_2 \frac{\ddot{x}}{r_2} &= r_2(T_3 - T_2) \\ \implies \frac{J_2}{r_2^2}\ddot{x} &= T_3 - T_2 \end{aligned} \tag{28}$$

Performing Eq. (27) + Eq. (28) gives

$$\begin{aligned} \frac{J_1}{r_1^2}\ddot{x} + \frac{J_2}{r_2^2}\ddot{x} &= T_1 - T_3 + T_3 - T_2 \\ \frac{J_1}{r_1^2}\ddot{x} + \frac{J_2}{r_2^2}\ddot{x} &= T_1 - T_2 \end{aligned} \tag{29}$$

And Eq. (29) + Eq. (23) gives

$$\left(m + \frac{J_1}{r_1^2} + \frac{J_2}{r_2^2}\right)\ddot{x} = -k_{\text{eff}}x \tag{30}$$

Finally,

$$\boxed{\underbrace{\left(m_{\text{cart}} + \frac{J_1}{r_1^2} + \frac{J_2}{r_2^2}\right)}_{m_e}\ddot{x} + k_{\text{eff}}x = 0} \tag{31}$$

If the pulleys are assumed to be uniform disks,

$$J_1 = \frac{1}{2}m_1 r_1^2, \quad J_2 = \frac{1}{2}m_2 r_2^2 \tag{32}$$

Substituting Eq. (32) into Eq. (31) gives

$$\boxed{\underbrace{\left(m_{\text{cart}} + \frac{1}{2}m_1 + \frac{1}{2}m_2\right)}_{m_e}\ddot{x} + k_{\text{eff}}x = 0} \tag{33}$$

In actuality, the equivalent mass in (33) should be larger than (31) since the pulleys aren't uniform disks due to the groove.

F Effective Mass Calculation

This section outlines the calculations used to determine the experimental effective mass of the system. The effective mass is determined by comparing the natural frequency of the no-measurement-system (whose mass is known) to the natural frequency of the measurement system (whose mass is unknown).

Suppose the natural frequency of the no-measurement-system for the small cart is $p_{\text{small, no sys}}$ and the natural frequency of the measurement system for the small cart is $p_{\text{small, sys}}$. Using the definition of resonance,

$$p_{\text{small, no sys}} = \sqrt{\frac{k_e}{m_{e_{\text{small, no sys}}}}}, \quad p_{\text{small, sys}} = \sqrt{\frac{k_e}{m_{e_{\text{small, sys}}}}}$$

$$\implies \frac{p_{\text{small, no sys}}}{p_{\text{small, sys}}} = \sqrt{\frac{m_{e_{\text{small, sys}}}}{m_{e_{\text{small, no sys}}}}}$$

$$\implies m_{e_{\text{small, sys}}} = \left(\frac{p_{\text{small, no sys}}}{p_{\text{small, sys}}}\right)^2 m_{e_{\text{small, no sys}}}$$

Table F.14: Natural Frequency Data from Free Vibration Trials

	Small Cart		Big Cart	
	w/o measuring system (Hz)	w/ measuring system (Hz)	w/o measuring system (Hz)	w/ measuring system (Hz)
Natural Frequency from Trials	1.1317	0.9096	0.8576	0.7513

Table F.15: Effective Mass Data

	Small Cart (kg)	Big Cart (kg)
Effective Mass from Trials	0.4099	0.5818
Effective Mass from Theory	0.4016	0.5833
Relative Error	2.09%	0.25%

Sample calculations will be shown for Table F.15. The effective mass of the small cart was found by using the natural frequency data from Table F.14. Then, knowing tha mass of the small cart is 0.2648 kg,

$$\begin{aligned} m_{e_{\text{small, sys}}} &= \left(\frac{1.1317}{0.9096}\right)^2 \times 0.2648 \\ &= \boxed{0.4099} \end{aligned}$$

The theoretical effective mass of the small cart is 0.4016 kg. The percent error is

$$\begin{aligned} \text{Percent Error} &= \frac{0.4099 - 0.4016}{0.4016} \times 100\% \\ &= \boxed{2.09\%} \end{aligned}$$

F.1 Effective Mass Error Analysis

Table F.16: Natural Frequency Error Data

w/ measuring system	Small Cart w/ measuring system	Big Cart
p (Hz)	0.9096	0.7513
δ_p (Hz)	0.009	0.016
δ_{m_e} (kg)	0.009	0.020

Sample calculations will be shown for Table F.16 for the small cart. The equation for m_e is

$$\begin{aligned} m_e &= \left(\frac{p_{\text{small, no sys}}}{p_{\text{small, sys}}}\right)^2 m_{e_{\text{small, no sys}}} \\ &= p^2_{\text{small, no sys}} p^{-2}_{\text{small, sys}} m^1_{e_{\text{small, no sys}}} \end{aligned}$$

This is the special case of the general formula for error propagation Eq. (21),

$$\begin{aligned} \delta_{m_e} &= \sqrt{\left((2)\frac{\delta_{p_{\text{small, no sys}}}}{p_{\text{small, no sys}}}\right)^2 + \left((-2)\left(\frac{\delta_{p_{\text{small, sys}}}}{p_{\text{small, sys}}}\right)^2\right) m_e} \\ &= \sqrt{\left((2)\frac{0.013}{1.1317}\right)^2 + \left((-2)\left(\frac{0.009}{0.9096}\right)^2\right) \times 0.2648} \\ &= \boxed{0.009} \end{aligned}$$

The error in the effective mass of the small cart is 0.009 kg. The error in the effective mass of the big cart is 0.020 kg.